Relationship of the pair creation yield during and after the interaction

- (1) Intense Laser Physics Theory Unit and Department of Physics Illinois State University, Normal, IL 61790-4560, USA
- (2) Key Laboratory for Laser Plasmas, School of Physics and Astronomy, Collaborative Innovation Center of IFSA, Shanghai Jiao Tong University, Shanghai 200240, China

We compare the predictions of two different approaches of studying the electron-positron pair-creation process triggered by a supercritical field inside the interaction region before the field is turned off. These two approaches are based on the projection of the electron-positron field operator on the sub-space spanned by either field-free or instantaneous energy eigenstates. For the case of an infinitely extended static electric field, we suggest that the type of the chosen turn-off of the external field determines which of the two approaches is physically more meaningful. We also derive an alternative quantum kinetic Vlasov equation, which is more meaningful than the traditional one to predict the interaction if the field is turned off sufficiently rapidly.

1

1. Introduction

The possibility to break down the vacuum state and to create electron-positron pairs from either a supercritical time-independent or a sufficiently rapidly oscillating external electromagnetic field has been the subject of recent interest. In part, this interest to probe the nonlinear properties of the quantum vacuum has also been fostered by dramatic advances in the development of lasers with unprecedented strength [1]. Here intensities of the order of 10^{24} $\sim 10^{26}$ W/cm² may become accessible in the next few years [2,3], which might open the door to exciting investigations of the vacuum decay via pair production.

Historically for a constant electric field the Dirac equation in external field can be solved exactly in terms of the parabolic cylinder functions [4] and all physical quantities such as the total number of produced pairs and their momentum distribution can be addressed. Certain exactly solvable models with explicit field switching on and off are also available. The observation that pairs are created mostly at rest in agreement with the previous studies, see original works [4-6] as well as monographs [7,8,9].

One of the long-term goals has been to obtain a better understanding of the fundamental aspects of the pair creation dynamics inside the creation region. However, despite some promising early works [10-12] it is presently still an unresolved problem how to appropriately and possibly even unambiguously identify particles inside the supercritical interaction zone. It therefore remains a conceptual challenge to relate the created "quasi-particles" during the interaction to the real particles after the interaction. This difficulty was also discussed in a nice work by the Moscow group [13]. While the space-time evolution of the electron-positron field operator can be obtained either as a solution to the time-dependent Dirac equation or equivalently as a solution from the Heisenberg equation of motion [7], how to separate this operator into an electronic and positronic portion in an unambiguous way is not clear. Computationally, it is therefore an important challenge to examine, which particular approach (meaning which subset of basis states are used for the projection of the field operator) is most suitable to predict the final (and uniquely determined) particles and their distributions after the interaction from the development of the corresponding quasi-particles during the interaction. In our opinion, to view the interaction zone from the very beginning as a theoretically inaccessible black box restricts a possibly important access to analyze the pair-creation process at those locations where it actually happens.

Let us take the point of view that for sufficiently long interaction times the effect of the turnoff on the final number of created particles after the interaction should be negligible as the
accumulated total number of created particles is large and most of the particles have left the
interaction zone. For these dynamical scenarios, the most meaningful approach to study the pair
creation process inside the interaction zone should be the one whose predictions for the particle
yield during the interaction should be easiest to be extrapolated to the true and unambiguous final
yield after the field is turned off. If in the long-pulse regime, the number of particles predicted
before and after the turn-off is very different, then the corresponding approach would be in
contradiction with our physical intuition.

There are also (at least) two mutually competing pair creation mechanisms during the turn-off time interval. While a very rapid turn-off obviously does not provide a sufficiently long duration for the particle number to grow, due to its rapid time-dependence, it's spectrum also provides new and large frequencies that could trigger (temporally induced) transitions, which by themselves could increase the yield. On the other hand, these high-frequency transitions are less important on a relative scale if the turn-off time is long, but then the particle number has also more time to grow. So there might be an optimal turn-off that would minimize the additional pair creation solely associated with the turn-off. In a similar vein, an early work by Gerry et al. [10] has studied the pair creation yield for the special case of a sub-critical and spatially localized electric field, where any pair-creation was possibly exclusively due to the temporal inhomogeneity provided during the field's turn-on and off periods. In case where the turn-on was immediately followed by the turn-off, the created particles did not have enough time to accelerate out of the pair creation zone and were completely annihilated again after the interaction. In contrast, if after the turn-on period the field was held constant, such that the electrons and positrons had sufficient time to separate spatially from each other, the turn-off period would further increase the particle yield. So the overall reducing or enhancing influence of the turn-off period on the final yield is determined, for subcritical fields, mostly by the duration of the plateau region.

In this work we examine the predictions of the pair-creation yield in supercritical fields for two different basis systems, based on the subspace of instantaneous eigenvectors of two different Hamiltonians. As both projections match when the external field is turned off, they naturally predict the same yield after the interaction. We will suggest that the type of chosen turn-off of the external field determines which projection during the interaction is more helpful with regard to predicting in a continuous way the final yield after the interaction. Even though from a

3

mathematically rigorous point of view, both projections are unphysical during the interaction, they can nevertheless provide a rough guidance to better understand the dynamics.

In order to amplify the differences for the two approaches, we examine an infinitely extended constant electric field as investigated in the pioneering work by Schwinger [14]. Here the interaction term, (given in the temporal gauge by the vector potential) grows linearly in time such that one can expect that the impact of the turn-off (which returns the potential back to zero) on the yield should be more pronounced for the yield than it is compared to more oscillatory time-dependent fields.

The work is organized as follows. In Section 2 we introduce the two projections on the electron-field operator, which allows us to revisit the Schwinger problem from the perspective of the dynamics of two-level systems. In Section 3 we show that the observation that each particle is born close to rest leads directly to an overall linear growth of the total particle yield. The observation that pairs are created mostly at rest in agreement with the excellent previous studies Narozhny and Nikishov [4]. In Section 4 we derive the corresponding quantum Vlasov equations for each projection. In Section 5 we suggest that the field's turn-off duration determines which approach to model the interaction is more physical. Finally, in Section 6 we finish with a brief summary and open questions.

2.1 The model system

If the external electric field does not have a spatial inhomogeneity, then the pair-creation dynamics can be described in the temporal gauge by a time-dependent vector potential A(t). For a one-spatial dimension dynamics, the Dirac Hamiltonian takes the form in atomic units

$$H = c \sigma_1 \left[P - \frac{qA(t)}{c} \right] + c^2 \sigma_3 \tag{2.1}$$

where P is the momentum operator and we assume the coupling to a positron with charge q = +1. The two 2×2 Pauli-matrices are denoted by σ_1 and σ_3 .

In this work we will examine two sets of basis states, the first set is based on the eigenstates of the force-free Hamiltonian, defined as $H_0|p;u\rangle = e_p|p;u\rangle$ and $H_0|p;d\rangle = -e_p|p;d\rangle$ with energy $e_p \equiv [c^4 + c^2p^2]^{1/2}$. The second set is generated by the instantaneous eigenstates of the full Hamiltonian, as discussed further below. For momentum p the spatial representation of the first

set is given by the two-component spinors, $\langle x|p;u\rangle=N$ { $[e_p+c^2]^{1/2}$, $[e_p-c^2]^{1/2}p/[p]$ } exp[ipx] and $\langle x|p;d\rangle=N$ { $-[e_p-c^2]^{1/2}p/[p]$, $[e_p+c^2]^{1/2}$ } exp[ipx], where N is the corresponding normalization factor. As the canonical momentum P is conserved, i.e. [P,H]=0, the external field can couple only states with the same momentum. In other words, only the pairs $|p;d\rangle$ and $|p;u\rangle$ are coupled at any time such that in this case the entire pair creation dynamics is equivalent to the collective dynamics of a set of infinitely many mutually independent two-level systems. We can therefore rewrite H as a sum of independent Hamiltonians over the momenta

$$H \equiv \sum_{p} [e_{p} | p; u \rangle \langle p; u | -e_{p} | p; d \rangle \langle p; d | -A(t) V_{dia} -A(t) V_{off}]$$
(2.2)

where the on- and off-diagonal couplings are given by

$$V_{dia}(t) \equiv \langle p; u | \sigma_1 | p; u \rangle | p; u \rangle \langle p; u | + \langle p; d | \sigma_1 | p; d \rangle | p; d \rangle \langle p; d |$$
(2.3a)

$$V_{\text{off}}(t) \equiv \langle p; d | \sigma_1 | p; u \rangle | p; d \rangle \langle p; u | + \langle p; u | \sigma_1 | p; d \rangle | p; u \rangle \langle p; d |$$
(2.3b)

Using the functional form of the energy eigenstates, the four matrix elements take the form $\langle p; u | \sigma_1 | p; u \rangle = c \ p/e_p \equiv a_p, \\ \langle p; d | \sigma_1 | p; d \rangle = -a_p \ \text{and} \\ \langle p; d | \sigma_1 | p; u \rangle = \langle p; u | \sigma_1 | p; d \rangle = c^2/e_p \equiv b_p. \\ \text{For a given momentum } p, \text{ the state is a superposition of the lower (subscript d) and upper (subscript u) level, } |\Psi_p(t)\rangle = C_{p;d}(t) \ |p; d\rangle + C_{p;u}(t) \ |p; u\rangle. \\ \text{The time-dependent amplitudes follow from the equation } \frac{i \ \partial |\Psi_p(t)\rangle}{\partial t} = H |\Psi_p(t)\rangle \text{ as}$

$$i\frac{dC_{p;u}(t)}{dt} = [e_p - A(t) a_p] C_{p;u}(t) - A(t) b_p C_{p;d}(t)$$
 (2.4a)

$$i\frac{dC_{p;d}(t)}{dt} = -A(t) b_p C_{p;u}(t) - [e_p - A(t) a_p] C_{p;d}(t)$$
 (2.4b)

As we will need it for below, let us perform a unitary transformation to another basis set [15], that is based on the instantaneous lower (D) and upper (U) energy eigenstates $|p; D_t\rangle$ and $|p; U_t\rangle$. These are defined based on the full Dirac-Hamiltonian, $H(t)|p; U_t\rangle = e_p(t)|p; U_t\rangle$ and $H(t)|p; D_t\rangle = -e_p(t)|p; D_t\rangle$, where the instantaneous energy eigenvalue takes the form $e_p(t) \equiv$

3/3/20

5

$$\begin{split} & \left[\left[e_p-A(t)\,a_p\right]^2+\left[A(t)\,b_p\right]^2\right]^{1/2}. \text{ For a fixed momentum p, the state } |\Psi_p(t)\rangle=C_{p;d}(t)\,|p;d\rangle\;+\\ & C_{p;u}(t)\,|p;u\rangle\,\text{can be equally expressed based on the superposition } |\Psi_p(t)\rangle=C_{p;D}(t)\,|p;D_t\rangle\;+\\ & C_{p;U}(t)\,|p;U_t\rangle. \text{ The corresponding expansion coeffcients } C_{p;D}\text{ and } C_{p;U}\text{ are given by the solution to} \end{split}$$

$$i\frac{dC_{p;U}(t)}{dt} = \alpha_p(t) C_{p;U}(t) + \beta_p(t) C_{p;D}(t)$$
 (2.5a)

$$i\frac{dC_{p;D}(t)}{dt} = \beta_p^*(t) C_{p;U}(t) - \alpha_p(t) C_{p;D}(t)$$
 (2.5b)

where the two matrix elements are given by

$$\alpha_{p}(t) = [[e_{p} - A(t) a_{p}]^{2} + [A(t) b_{p}]^{2}]^{1/2}$$
(2.5c)

$$\beta_{p}(t) = i \frac{dA}{dt} c^{2} / [2 \alpha_{p}(t)^{2}]$$
 (2.5d)

2.2 Definition of particles during the interaction

We can use any complete basis set to represent the electron-positron field operator $\Psi(x,t)$ by introducing the positronic (electronic) annihilation operators b_p (d_p). The particular choice of the basis states automatically defines the meaning of these fermionic operators. For example, if we arbitrarily choose the field-free eigenstates $|p;u\rangle$ and $|p;d\rangle$ of H_0 introduced above, then, when acting on the field-free vacuum state, the operator b_p^{\dagger} would create an excitation of the mode $|p;u\rangle$, while d_p^{\dagger} would create an excitation of the mode $|p;d\rangle$. The conceptual problem [16] is to split this operator into two portions in order to represent its positronic and electronic parts, i.e., $\Psi(x,t) = \Psi_{pos}(x,t) + \Psi_{ele}(x,t)$. Before and after the external field is present, this separation is undisputed, for example, the positronic portion can be obtained by projecting the full operator $\Psi(x,t)$ onto the sub-space of positive energy states via $\Psi_{pos}^{(0)}(x,t) \equiv \sum_p |p;u\rangle\langle p;u| \Psi(x,t)$, leading to $\Psi_{pos}^{(0)}(x,t) = \sum_p b_p(t)\langle x|p;u\rangle$. In this case, the resulting total number of created positrons after the interaction can be calculated from the quantum field theoretical expectation value as $N^{(0)}(t) \equiv \langle \Psi_{pos}^{(0)}(t)^{\dagger} \Psi_{pos}^{(0)}(t)\rangle$, leading to $N^{(0)}(p,t) \equiv \langle b_p(t)^{\dagger} b_p(t)\rangle = |C_{p;u}(t)|^2$ and, for the total number of positrons, to $N^{(0)}(t) \equiv \sum_p \langle b_p(t)^{\dagger} b_p(t)\rangle = \sum_p |C_{p;u}(t)|^2$. However, to interpret

 $\langle \Psi_{pos}^{(0)}{}^{\dagger} \Psi_{pos}^{(0)} \rangle$ with the number of positrons during the interaction is not unambiguous, as we could have equally chosen a different sub-space for the corresponding projection.

For example, we could have also defined the positronic portion as $\Psi_{pos}^{(1)}(x,t) \equiv \sum_p |p;U_t\rangle\langle p;U_t|$ $\Psi(x,t)$ based on the instantaneous eigenvectors of the full Dirac-Hamiltonian H(t) as introduced in Sec. 1.1. In this case, the corresponding particle numbers would be calculated differently, i.e., $N^{(1)}(t) \equiv \langle \Psi_{pos}^{(1)}(t)^\dagger \Psi_{pos}^{(1)}(t) \rangle$, leading here to $N^{(1)}(p,t) \equiv \langle B_p(t)^\dagger B_p(t) \rangle = |C_{p;U}(t)|^2$ and, for the total number of positrons, to $N^{(1)}(t) \equiv \sum_p |C_{p;U}(t)|^2$. One of the main goals of this article is to compare the different predictions based on $\Psi_{pos}^{(0)}(t)$ and $\Psi_{pos}^{(1)}(t)$ We suggest that the type of turn-off determines which projection is physically more meaningful during the interaction to predict the final outcome after the interaction.

3. The two-level system dynamics and the relationship to the long-time pair creation rate

In Section 3.1 we examine the time-evolution for $N^{(0)}(p,t)$ and $N^{(1)}(p,t)$ for a constant electric field. In Section 3.2 we will discuss the relationship between the temporal growth of the particle density N(p,t) for a positron with momentum p and the resulting total number of all positrons N(t), obtained by summing over all momenta.

3.1 Analysis of N⁽⁰⁾(p,t)

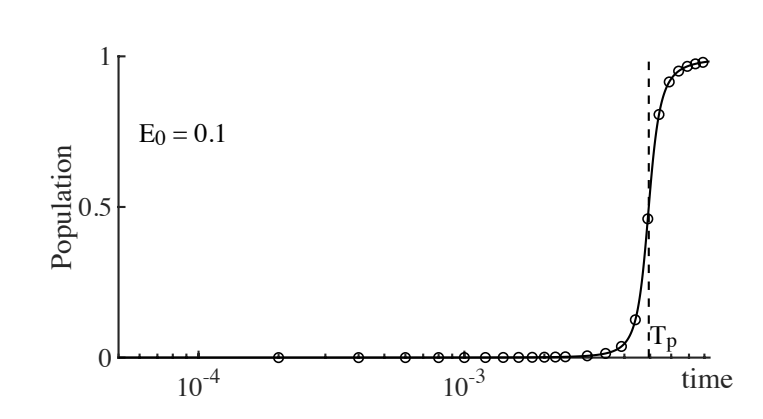
From now on we assume that the electric field strength is constant in time and denoted by E_0 , i.e. A(t) = -c E_0 t and it is switched on at t=0. Here it is important to note that due to the nonvanishing diagonal terms A(t) a_p in Eq. (2.4), the particular interaction shifts the energies $\pm e_p$ to their instantaneous diagonal elements $\pm [e_p + c$ E_0 t $a_p]$. As the sign of the coefficients a_p is determined by the sign of the momentum p, we expect that the manifolds for positive and negative momentum will show entirely different responses to the field. This symmetry breaking is, of course, directly associated with the orientation of the electric field vector that was chosen positive, such that positrons are accelerated to the right. Positrons with positive energy and positive momentum would be accelerated, while those that move initially to the left (p<0) would be slowed down, brought to rest and then gain a positive velocity.

For states with negative energy $-e_p$ the sign of the canonical momentum p is opposite to the actual velocity v, i.e. $v = \frac{dH}{dp} = -cp/e_p$. In this case the speed of states with negative momentum is increased even further by the field, while states with positive momentum (moving initially to the left) would be slowed down first.

This asymmetry has interesting implications. For negative momenta p, there is a characteristic time duration, denoted by T_p , after which the two instantaneous energies $\pm e_p(t)$ become equal to each other, i.e., $e_p - A(T_p)a_p = -[e_p - A(T_p)a_p]$. Using $A(t) = -c E_0 t$, we obtain

$$T_{p} = -\frac{e_{p}^{2}}{c^{2}E_{0}p} = -(m^{2}c^{2} + p^{2})/(E_{0}p)$$
(3.1)

During time intervals centered at time T_p we will have a momentary degeneracy and we would expect a maximum transfer of the population from the lower to the upper level to occur at those times. This expectation for $N^{(0)}(p,t)$ is confirmed by the numerical data as we show in Figure 1 for four different electric field strength E_0 .



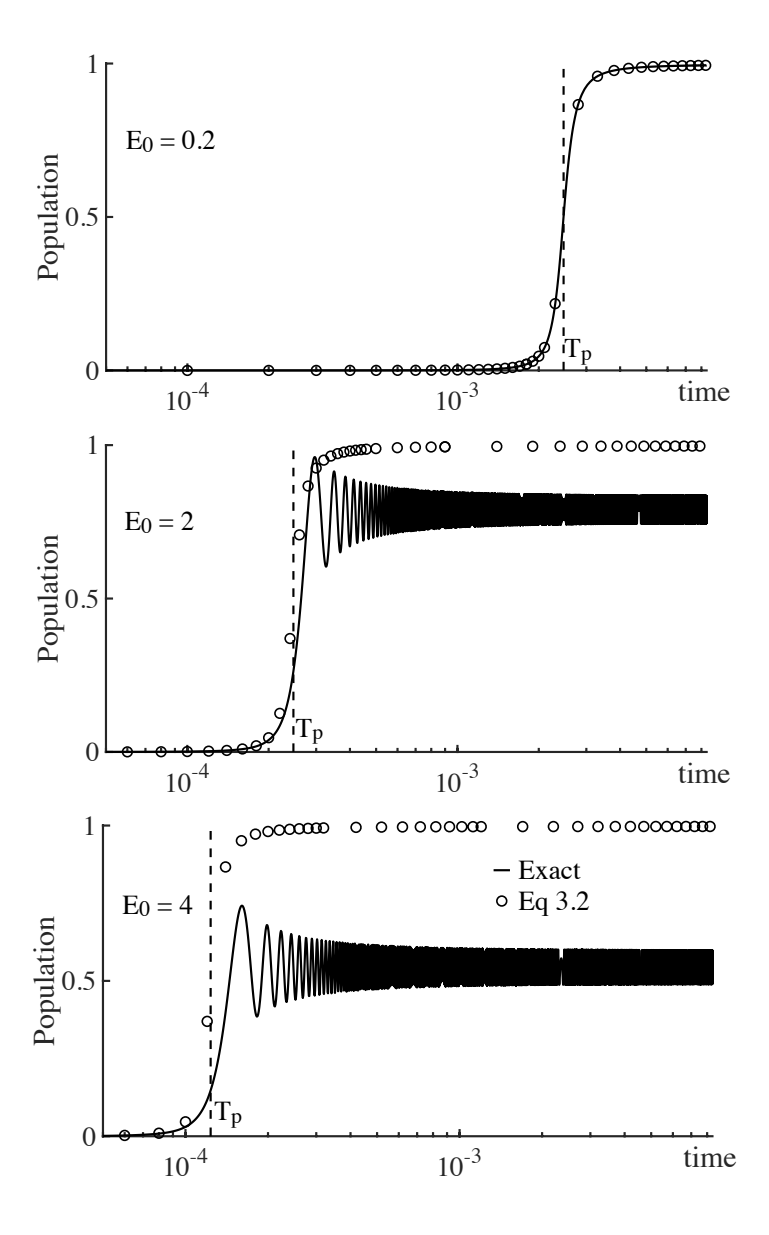


Figure 1 The population of the upper level $|C_{p;u}(t)|^2$ as a function of time during the interaction with four different electric fields with amplitude E_0 (in units of c^3). For comparison, the open circles for each case correspond to the analytical formula given by Eq. (3.2). The four dashed vertical lines are the times of perfect energy degeneracy T_p . [The time is in atomic units, and we chose momentum $p = -200 \ (2\pi/L)$, with $L = 1 \ a.u.$]) Note the circles and the straight lines correspond to different quantities (actual pair creation in the "free" particle representation and the "free" particle content of an "adiabatic" state).

Here the four vertical lines point towards the predicted center of the population transition windows according to Eq. (3.1) for each E₀. The agreement between T_p and the true transition time is excellent.

For large values of p, the pair-creation time approaches $T_p = -p/(E_0)$. This has interesting implications with regard to the velocity the particles take at their very birth moment. In the

temporal gauge, the (relativistic) velocity of the particles is given by $\frac{dx}{dt} = c^2(p + E_0 t)[c^4 + c^2(p + E_0 t)^2]^{-1/2}$, which, when being evaluated at $t = T_p$, is identical to zero. This suggests that it is most likely that, in a spatially homogeneous electric field, the particles are born at rest, before they get accelerated consecutively by the same field.

Furthermore, the data suggest that there are two distinct regimes depending on the magnitude of the electric field E_0 . For small amplitudes, we enter the adiabatic regime [17-19]. Adiabaticity assumes in general that the external field changes slowly enough, such that the instantaneous eigenvectors of the time-dependent Hamiltonian, defined as $H(t) | p; U_t \rangle = e_p(t) | p; U_t \rangle$, become dynamically meaningful. In other words, if the initial state happens to agree with an eigenstate of H(t=0), then the truly time-evolved state is (up to an irrelevant overall phase) identical to the instantaneous eigenvector. In our case, the initial state $\{C_{p;u}(t=0), C_{p;d}(t=0)\} = \{0,1\}$ matches one of the two eigenvectors of H(t=0) (with energy $-e_p$). If we take the square of the upper component of the state $|p;U_t\rangle$, we obtain

$$|C_{p;u}(t)|^2 = A(t)^2 b_p^2 / [b_p^2 A(t)^2 + \{e_p - a_p A(t) + [e_p^2 - 2 e_p a_p A(t) + A(t)^2]^{\frac{1}{2}}\}^2]$$
(3.2)

This function begins at zero and approaches asymptotically the final population

$$|C_{p;u}(t \to \infty)|^2 = \frac{b_p^2}{2a_p + 2} = (1 - \frac{cp}{e_p})/2$$
 (3.3)

This expression allows us to determine the efficiency of the adiabatic population transfer for each two-level system. As the amount of the (negative) momentum increases, this final population grows monotonically from $|C_{p;u}(t\to\infty)|^2=0.5$ (for p=0) to $|C_{p;u}(t\to\infty)|^2=1$ for very large (negative) momenta. If we introduce a dimensionless time $\tau\equiv E_0$ t/c, then the upper population is solely a function of τ , i.e., A(t)=-c E_0 $t=-c^2$ τ , in this adiabatic regime. The open circles in Figure 1 represent the predictions of Eq. (3.2), which agree perfectly with the actual data for sufficiently small E_0 . The non-adiabatic regime is analytically less accessible. It is characterized by a heavily oscillatory long-time behavior of the population in the upper state.

3.2 From N(p,t) to N(t)

For sufficiently long times, we would expect that, during the interaction, the total number of created (quasi) particles should increase linearly with time, permitting us to describe the yield by a single rate constant, i.e. $N(t) = \Gamma$ t. In this section, we will show how this linear growth rate Γ can be derived from the asymptotic values for $N^{(0)}(p,t)$ and $N^{(1)}(p,t)$ associated with each two-level system. We will show that the rate [associated with $N^{(0)}(t)$] amounts to $\Gamma^{(0)} = L \frac{E_0}{2\pi}$ for small E_0 and the rate [associated with $N^{(1)}(t)$] amounts to a substantially smaller amount, $\Gamma^{(1)} = L \frac{E_0}{2\pi}$ $Exp[-\pi c^3/E_0]$. The linear increase of the total number of created particles with the physical extension of the system L in each case is expected for the one (spatial) dimensional dynamics.

In Eq. (3.3) we saw that for long times and sufficiently small E_0 , $N^{(0)}(p,t)$ approaches a value close to unity, corresponding to a nearly complete transfer of population to the upper state. However, for larger electric fields, the asymptotic behavior for $N^{(0)}(p,t)$ was oscillatory and with maxima that were smaller than 1. At first, this seems to contradict with the intuitively expected behavior that the final yield should increase monotonically with the strength of the electric field. However, we will show now that the total yield (for which we expect a linear increase in time for long times), does indeed grow with increasing E_0 as well.

If we assume that the time duration required for the population transfer is very short, neglect the actual couplings facilitated by the off-diagonal terms A(t) b_p , and furthermore assume that the entire population is transferred completely at T_p to the upper level (see Figure 1 for small E_0), then the total population for all momenta can be very crudely approximated by

$$\sum_{p} |C_{p;u}(t)|^2 = \sum_{p} \theta(t - T_p)$$
(3.4)

where the summation extends over all negative momenta that can be labeled by $p = n \Delta p$ (n=0, -1, -2, -3 ..) with an effective mode spacing Δp that depends on the extension L of the system, $\Delta p = 2\pi/L$.

We therefore arrive at the following interesting physical picture for the Schwinger paircreation mechanism viewed from the perspective of a set of two-level systems. Each positron with a given momentum p is created only at unique time given by $T_p = -(m^2c^2 + p^2)/(E_0\,p)$. As this time is shortest for p = -mc, those positrons are created first and after a delay time $T = (2mc)/E_0$. For positrons with large momenta we have $T_p \approx -\frac{p}{E_0} = -n\,\Delta p/E_0$. Therefore the momenta are created consecutively in time. Using $\sum_n \theta(t-\kappa n) \approx t/\kappa$ we can approximate Eq. (3.4) as

$$\sum_{p} |C_{p;u}(t)|^2 \approx \left(\frac{E_0}{\Delta p}\right) t = L \frac{E_0}{2\pi} t$$
 (3.5)

leading to the expected linear growth in time. Our simplified model based on $\Psi^{(0)}_{pos}(t)$ therefore predicts a pair-creation rate per unit length given by $\gamma = \frac{E_0}{2\pi}$.

A very similar analysis can also be performed for the solution to the two-level system of Eqs. (2.5) based on the instantaneous eigenstates. Here the off-diagonal couplings are given by $\beta_p(t)$, which are also time-dependent, but in contrast to $A(t)b_p$, they vanish in the limit of infinite times. However, they take their maximum value at precisely the same time T_p [see Eq. (3.1)] when the diagonal elements e_p – $A(t)a_p$ in Eq. (2.4) vanish. In other words, both projections predict consistently that quasi-particles with momentum p are solely created close to the time T_p .

While the transition to the upper level happens at precisely the same time window as given by Eq. (3.1), here the population transfer based on $\alpha_p(t)$ and $\beta_p(t)$ is not complete. In fact, we find that the asymptotic value for $N^{(1)}(p,t)$ is numerically indistinguishable from $N^{(1)}(p,t) \to \text{Exp}[-\pi c^3/E_0]$. This (in E₀) non-perturbative expression can also be derived from the corresponding Landau-Zener transition rate [17], as reported, e.g., in the excellent article by Wittig [18], or, from an alternative approach based on the asymptotic properties of the Weber functions (parabolic cylinder functions). As a result, here prediction of corresponding rate for the total number of created particles would amount to $\Gamma^{(1)} = L \frac{E_0}{2\pi} \text{Exp}[-\pi c^3/E_0]$. The linear part is therefore associated with the scaling of the birth moments with E₀, while the exponential cofactor reflects the incomplete adiabatic transfer.

To avoid a possible confusion, we should point out that $\Gamma^{(0)} = L \frac{E_0}{2\pi}$ is strictly correct only for small E_0 , while $\Gamma^{(1)}$ takes (coincidentally) the same form only in the limit for very large E_0 .

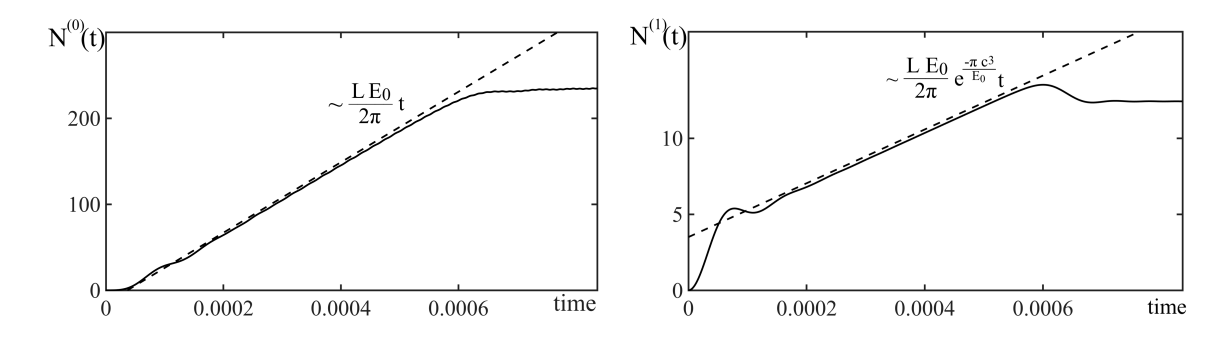


Figure 2 The time-dependence of the total number of created positrons with momentum between p = -250 ($2\pi/L$) and 250 ($2\pi/L$) based on the projections leading to N⁽⁰⁾(t) and N⁽¹⁾(t). For comparison, the dashed lines have the slopes L E₀/(2 π) and L E₀/(2 π) Exp($-\pi$ c³/E₀). [E₀ = 1 c³, the time is in atomic units and L = 1 a.u.]

In order to test these theoretical ideas, in Figure 2 we have computed $N^{(0)}(t)$ and $N^{(1)}(t)$ by summing over the contributions of 500 two-level systems with momenta ranging from p = -250 $(2\pi/L)$ to 250 $(2\pi/L)$ (for L=1). For early times, both graphs grow quadratically, associated with the abrupt turn on of the vector potential at time t=0. After a characteristic time interval of the order of $T_0 = 2\pi/(2c^2)$, which is about 1.67×10^{-4} a.u., both graphs evolve into the expected linear growth regime. For comparison, we have indicated by the dashed lines the corresponding slopes L E₀/(2 π) and L E₀/(2 π) Exp[- π c³/E₀]. The agreement is superb. After a time of about 6×10⁻⁴ a.u. the linear growth stops, as this time corresponds to T_p for the largest momentum that we have included in the calculation for N(t).

To examine the importance of positive momenta, we have repeated the simulation by excluding their contributions. As expected, these momenta contribute only to the early time behavior of N(t) for both projections and have no impact on the final rate.

4. Quantum kinetic transport equations for $N^{(0)}(p,t)$ and $N^{(1)}(p,t)$

As numerous studies in the literature of spatially homogeneous electric fields use the quantum Vlasov equation [13,20-25] for the total number of created particles $N^{(1)}(p,t)$, we point out here briefly that a similar equation can also be derived for $N^{(0)}(p,t)$. The time-evolution of both projections can be obtained equivalently from either the corresponding two-level equations based on complex amplitudes, see Eq. (2.4) and Eq. (2.5) in Section 2, which have formally the same general structure

3/3/20

$$i \frac{dc_{+}(t)}{dt} = D(t) c_{+}(t) + B(t) c_{-}(t)$$
 (4.1a)

$$i \frac{dc_{-}(t)}{dt} = B^{*}(t) c_{+}(t) - D(t) c_{-}(t)$$
(4.1b)

In order to eliminate the diagonal couplings, we introduce $C_{+}(t) \equiv c_{+}(t) \exp[-i\theta(t)]$ and $C_{-}(t) \equiv c_{-}(t) \exp[i\theta(t)]$, where the phase is defined as $\theta(t) \equiv \int_{-t}^{t} d\tau D(\tau)$. This leads to the equations,

$$i \frac{dC_{+}(t)}{dt} = B(t) \exp[i 2\theta(t)] C_{-}(t)$$
 (4.2a)

$$i \frac{dC_{-}(t)}{dt} = B^{*}(t) \exp[-i 2\theta(t)] C_{+}(t)$$
 (4.2b)

The main quantity of interest is the population in the upper level, $\rho(t) \equiv |c_+(t)|^2 = |C_+(t)|^2$. Since $d\rho/dt = d$ [$C_+(t)^*$ $C_+(t)$]/dt = d $C_+(t)^*$ /dt $C_+(t) + C_+(t)^*$ d $C_+(t)$ /dt, we may use (4.2a) and its complex conjugated form to show that $d\rho/dt = 2$ Re{B(t) exp[i2 $\theta(t)$] $C_+^*(t)$ $C_-(t)$ }. To relate the right-hand side with the left-hand side, we need to find the equation of motion for $C_+^*C_-$ and to see how it varies with ρ . Since d [$C_+^*(t)$ $C_-(t)$]/ $dt = dC_+^*(t)$ /dt $C_-(t) + C_+^*(t)$ $dC_-(t)$ /dt, we use the complex conjugated form of Eq. (4.2a) and Eq. (4.2b) and $C_-^*(t)$ $C_-(t) = 1 - C_+^*(t)$ $C_+(t)$ to obtain $d/dt[C_+^*C_-] = B^*(t)$ exp[$-i2\theta(t)$](1 -2ρ). This equation can be integrated in time, leading to $C_+^*C_-(t) = \int^t d\tau$ $B^*(\tau)$ exp[$-i2\theta(\tau)$][$1-2\rho(\tau)$], where we have incorporated the initial condition [$C_+^*C_-(t) = 0$]. Finally, we insert $C_+^*C_-(t)$ back into the differential equation for ρ . As B is either a real or purely imaginary function of time, B(t) B*(τ) is real, the real part of the remaining expression is easily found. As a result, we obtain

$$\frac{d\rho}{dt} = 2 B(t) \int_{0}^{t} d\tau B^{*}(\tau) \cos[2\theta(t) - 2\theta(\tau)][1 - 2\rho(\tau)]. \tag{4.3}$$

The factor $1-2\rho$ on the RHS of Eq.(4.3) reflects the fact that the kinetic equation contains contributions of both the "gain" (pair creation from the vacuum itself) as well as the "loss"

(inverse process of pair annihilation into vacuum) represented by the factors $1-\rho$ and ρ , respectively.

If ρ in Eq. (4.3) is equal to $|c_{p,u}|^2$, then the couplings are $B(t)=-b_p$ A(t) and $\theta(t)\equiv\int^t d\tau \ [e_p-a_p\ A(\tau)]$. For the special case of a homogeneous electric field this leads to $B^{(0)}(t)=-c\ b_p$ E_0 t and $\theta^{(0)}(t)\equiv\int^t d\tau \ [e_p+a_p\ c\ b_p\ E_0\ \tau]=e_p\ t+a_p\ c\ b_p\ E_0\ t^2/2$. On the other hand, if ρ is equal to $|c_{p,U}|^2$, then $B(t)=i\ dA/dt\ c^2/\left[2\ [e_p-A(t)a_p]^2+[A(t)b_p]^2\right]$ and $\theta(t)\equiv\int^t d\tau\ \left[[e_p-A(\tau)a_p]^2+[A(\tau)b_p]^2\right]^{1/2}$. For the homogeneous field this leads to $B^{(1)}(t)=-i\ E_0\ c^3/\left[2\ [e_p+E_0\ t\ c\ a_p]^2+[E_0\ t\ c\ b_p]^2\right]$ and $\theta^{(1)}(t)\equiv c^3/(2E_0)\left\{(E_0\ t/c+p/c)[1+(E_0\ t/c+p/c)^2]^{1/2}+Sinh^{-1}(E_0\ t/c+p/c)\right\}$.

The two associated phase factors $\theta^{(0)}(t)$ and $\theta^{(1)}(t)$ evolve rather differently. For short interaction times, $\theta^{(0)}(t)$ grows linearly in time with rate e_p , while the other phase $\theta^{(1)}(t)$ starts with the non-zero value $\theta^{(1)}(t=0) = [p\ e_p + c^3\ Sinh^{-1}(p/c)]/(2E_0)$, which diverges (for non-zero momentum) in the limit of small electric field amplitudes E_0 . It then grows linearly with the same rate e_p . This possible divergence suggests that for short interaction times the corresponding kinetic transport equation for $N^{(0)}(p,t)$ might be computationally easier to handle than the traditional one for $N^{(1)}(p,t)$. In the long-time limit, both phases grow quadratically in time, i.e., $\theta^{(0)}(t) \to E_0 \ p\ t^2/2\ (c^2/e_p)$ and $\theta^{(1)}(t) \to E_0 \ p\ t^2/2\ (c^2/e_p)^2$, respectively.

As solving the integro-differential equation directly for $\rho(t)$ is difficult, it is customary to introduce two auxiliary functions G and H, with $G(t) \equiv \int^t d\tau \ B^*(\tau) \cos[2\theta(t) - 2\theta(\tau)] \ [1 - 2\rho(\tau)]$ and $H(t) \equiv \int^t d\tau \ B^*(\tau) \sin[2\theta(t) - 2\theta(\tau)] \ [1 - 2\rho(\tau)]$. With these functions, Eq. (4.3) can be equally expressed as three coupled ordinary differential equations

$$\frac{\mathrm{d}\rho}{\mathrm{d}t} = 2 \mathrm{B(t)} \mathrm{G(t)} \tag{4.4a}$$

$$\frac{dG}{dt} = 2 B(t) [1 - 2\rho(\tau)] - 2 \frac{d\theta}{dt} H(t)$$
 (4.4b)

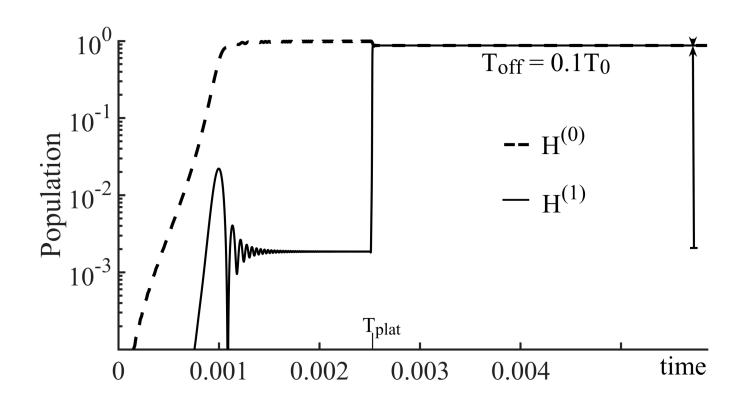
$$\frac{dH}{dt} = 2 G(t) \tag{4.4c}$$

These equations are solved with the initial condition $\rho(0) = G(0) = H(0) = 0$. The two projections correspond to the same Eq. (4.4), except for the different functions of B and θ .

5. Comparison of both projections including the turn-off of the field

We should note that the analysis above has examined the time-evolution *during* the interaction and we have seen that the two projections of the electron-positron field operators lead to rather different predictions. While it is interesting to note that both descriptions predict the identical birth moments for the corresponding quasi-particles, they predict entirely different rates for the asymptotic growth of the particles yield and the important question arises which approach has more predictive power with regard to the real particles after the interaction.

As the field was assumed to be spatially homogeneous, the created particles cannot be accelerated out of the interaction zone and we therefore can only examine this question by turning the field off in time. Except a few special temporal pulse shapes for which the quantum Vlasov equation can be solved exactly [26], the determination of the final yield after the interaction is more difficult to predict based on solely analytical approaches. In our computational analysis we have turned the field off after a plateau time (denoted by T_{plat}) during which the electric field was constant, i.e. $A(t) = -c E_0 t$, by multiplying the vector potential with the exponential decaying factor $Exp[-(t-T_{plat})/T_{off})$, for $T_{plat} < t$. The turn-off duration T_{off} was varied from zero (corresponding to an abrupt turn-off) to arbitrary long intervals. As during the turn-off period, the particles continue to be created (even though with decreasing rates), we should mention numerous works [27-29] that have shown that any truly adiabatic turn-off (corresponding to an infinite T_{off}) can lead to an infinite number of created particles.



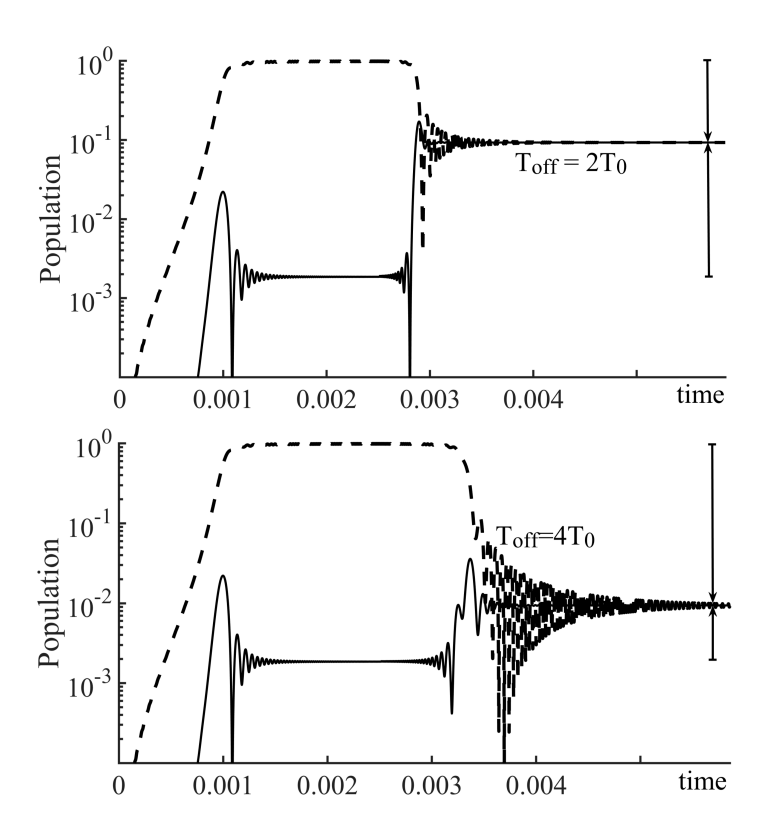


Figure 3 The time-dependence of the population of the upper level $|C_{p;u}(t)|^2$ (based on $H^{(0)}$, dashed line) and $|C_{p;U}(t)|^2$ (based on $H^{(1)}$, continuous line) for three different turn-off durations T_{off} . The field was turned on abruptly and the turn-off begins after a (in-field) plateau time $T_{plat} = 15 \ T_0$, where $T_0 = 2\pi/(2c^2)$. To guide the eye the vertical arrows are the mismatch between the (in-field) plateau and final population after the turn-off. The total interaction time displayed was $T = 35 \ T_0$. [Momentum $p = -200 \ (2\pi/L)$ and the electric field amplitude was $E_0 = 0.5c^3$]

In Figure 3 we graph the populations $N^{(0)}(p,t)$ and $N^{(1)}(p,t)$ as a function of time for three different turn-off durations T_{off} . In each of the six cases, the field was constant $(E_0=0.5c^3)$ for a time $T_{plat}=15~T_0$, with the unit of time $T_0=2\pi/(2c^2)$. As both projections are identical when the field vanishes, the final populations corresponding to the real particles are identical for both approaches, $N^{(0)}(p,t\to\infty)=N^{(1)}(p,t\to\infty)$. However, the particular approach to this final particle number is drastically different. For short turn-off times, the final yield is much better predicted by $N^{(0)}(p,t)$ than by $N^{(1)}(p,t)$. For example, for $T_{off}=0.1~T_0$, the plateau value $N^{(0)}(p,t)=0.997$ during the interaction reduces only to $N^{(0)}(p,t\to\infty)=0.985$, whereas as the plateau value for $N^{(1)}(p,t)=0.00186$ (a value close to $Exp[-\pi c^3/E_0]=0.00187$) has to increase by a huge factor of 547 to predict the same asymptotic value. As in our opinion the number of particles should not be able to grow so drastically during the ramping off of the field, we suggest that the projection

3/3/20

leading to $N^{(0)}(p,t)$ is physically more meaningful to describe the dynamical features such as the yield and spatial probability distributions during the interaction.

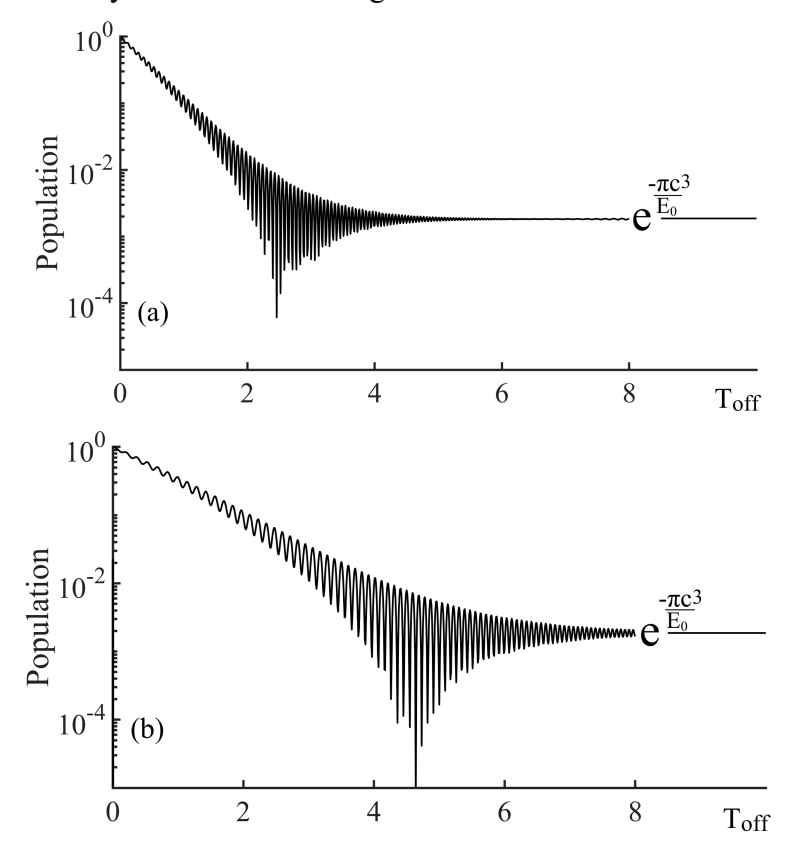


Figure 4 The final population of the upper level as a function of the turn-off duration $T_{off.}$ The field was turned off after a time $T_{plat}=15~T_0$, where $T_0=2\pi/(2c^2)$. (a) $p=-100~(2\pi/L)$ and (b) $p=-200~(2\pi/L)$. [Electric field $E_0=0.5c^3$ and L=1~a.u.]

In order to examine in more detail how the duration of the turn-off can be used to control the *final* population, we have graphed in Figure 4 the final values $N^{(0)}(p,t\to\infty)=N^{(1)}(p,t\to\infty)$ as a continuous function of T_{off} for two different momenta. We chose an electric field $E_0=0.5c^3$, for which the final population in the special case of $T_{off}=0$ was close to unity. The plateau time was chosen sufficiently long such that the asymptotic value during the interaction was reached for each momentum, i.e. $T_p < T_{plat}$. We find that the final population decreases non-monotonically with T_{off} , but approaches a final value that is close to $Exp[-\pi c^3/E_0]$, independent of the momentum. Furthermore, the required turn-off time to actually reach this "truly adiabatic" turn-off yield seems to increase with the momentum p.

6. Summary and open questions

For the case of a constant electric field we have compared the temporal growth of the created number of positrons during the interaction for two approaches based on different projections of the electron-positron field operator. Both approaches predict consistently that for a given momentum the positrons are produced only during a short time window, which is determined by the electric field and the momentum of the positrons. Together with the observation that for a positive electric field only positrons with negative momenta contribute to the long-time yield, this has interesting consequences. It turned out, that particles are born most likely at rest (with energy mc²) and they accumulate higher energies only as they get accelerated by the field.

In order to examine which of the two projections is in general more meaningful to illuminate the dynamics during the interaction, we have compared their extrapolated predictions for the yield after the interaction. If we adopt the view that due to the additional interaction time provided by the turn off process, the pair creation yield should always continue to increase from its particular plateau value (before the turn-off begins), then the projection based on the instantaneous eigenvectors of the full Dirac Hamiltonian seems to be more physical. On the other hand, for nearly abruptly turned off fields, the yield predicted by the projection based on the field-free states evolves much more smoothly to the final value and is therefore more beneficial.

We noted that for small electric fields, the growth pattern of $N^{(0)}(p,t)$ was numerically well described by a simple analytic adiabatic model according to Eq. (3.2). It turns out that if we subtract this analytical prediction from the exact numerical data, the difference is remarkably close to the prediction based on the other projection, leading to $N^{(1)}(p,t)$. This is advantageous as it suggests that for each momentum the data for $N^{(0)}(p,t)$ and $N^{(1)}(p,t)$ can be related to each other through Eq. (3.2), but certainly more systematic studies for wider parameter ranges are required.

While (at least for small E_0) the adiabatic analysis permitted us to predict $N^{(0)}(p,t)$ with good accuracy, using a similar adiabatic approach to approximate $N^{(1)}(p,t)$ was not so helpful. In fact, expanding the two-level amplitudes with regard to the instantaneous eigenvectors of the Hamiltonian given by $\{\{\alpha_p(t),\beta_p(t)\},\{\beta_p(t),-\alpha_p(t)\}\}\$ led to predictions qualitatively similar to those of $N^{(0)}(p,t)$.

For conceptual and computational simplicity, the analysis was performed for a onedimensional geometry, in other words, we limited the canonical momenta to a direction that was (anti-) parallel to the applied electric field. The inclusion of other momenta along a direction that is perpendicular to the E-field does not affect any general conclusion of this work nor does it provide new insight, even thought the final rates have a functionally different form due to the required additional integration over those neglected degrees of freedom. In a realistic 3+1 dimensional analysis one can also account for both spin directions.

While the study of an infinitely extended and temporally constant electric field led to the pioneering work of Schwinger [14], from an experimental point of view, explorations on external field with space-time dependencies are more advantageous. If the field is oscillatory then the actual differences between the two projections leading to the two different Vlasov equations might be much less significant and therefore a description of the dynamics inside the supercritical interaction zone might be less controversial. But it certainly remains an open theoretical challenge for future work.

Acknowledgements

S.D. and R.F. would like to thank ILP for the nice hospitality during their visits to Illinois State. R.F. acknowledges the support by the exchange program of Illinois State University and ITESM of Mexico. S.D. acknowledges the China Scholarship Council program. We acknowledge stimulating discussions with Drs. Q. Wang, L.B. Fu and J. Liu about the quantum Vlasov equation for periodic fields. This work has been supported by the NSF, NSFC (Grants No. 11529402 and No. 11721091) and Research Corporation.

References

- [1] For a comprehensive review, see A. Di Piazza, C. Müller, K.Z. Hatsagortsyan and C.H. Keitel, Rev. Mod. Phys. 84, 1177 (2012) or a more recent one, see, B.S. Xie, Z.L. Li, S. Tang, Matter and Radiation at Extremes 2, 225 (2017).
- [2] G.A. Mourou, T. Tajima and S.V. Bulanov, Rev. Mod. Phys. 78, 309 (2006).
- [3] For recent advances in high power laser systems, see, for example, the websites of the following labs: ELI (Paris), diocles (Lincoln), xfel (Hamburg), sparc (Darmstadt), Vulcan, HiPER and Astra Gemini (Oxfordshire), polaris (Jena) or Shenguang III (Mianyang), LCLS (Stanford), TPL (Austin) or numerous references in https://eli-laser.eu/.
- [4] Narozhny & Nikishov, Sov. J. Nucl. Phys. 11, 596 (1970).
- [5] E. Brezin and C. Itzykson, Phys. Rev. D 2, 1191(1970).
- [6] V. S. Popov, JETP Lett. 13, 185 (1971); Sov. Phys. JETP 34, 709 (1972).
- [7] W. Greiner, B. Müller, and J. Rafelski, "Quantum Electrodynamics of Strong Fields (Springer-Verlag, Berlin, 1985).
- [8] A. A. Grib, S. G. Mamaev, and V. M. Mostepanenko, "Vacuum Quantum Effects in Strong Fields" (Atomizdat, Moscow, 1988) (republished by Friedmann Laboratory, St. Petersburg, 1994).
- [9] E. S. Fradkin, D. M. Gitman, and Sh. M. Shvartsman, "Quantum Electrodynamics with Unstable Vacuum" (Springer-Verlag, Berlin, 1991).
- [10] C.C. Gerry, Q. Su and R. Grobe, Phys. Rev. A 74, 044103 (2006).
- [11] R. Dabrowski and G.V. Dunne, Phys.Rev. D90, 025021 (2014) and Phys. Rev. D 94, 065005 (2016).
- [12] O.Z. Lv, J. Unger, Y.T. Li, Q. Su and R. Grobe, Euro. Phys. Lett. 116, 40003 (2016).
- [13] A.M. Fedotov, E.G. Gelfer, K. Yu. Korolev and S.A. Smolyansky, Phys. Rev. D 83, 025011 (2011).
- [14] J.S. Schwinger, Phys. Rev. 82, 664 (1951).
- [15] G.R. Mocken, M. Ruf, C. Müller and C.H. Keitel, Phys. Rev. A 81, 022122 (2010).
- [16] P. Krekora, Q. Su and R. Grobe, Phys. Rev. A 73, 022114 (2006).
- [17] C. Zener, Proc. Royal Soc. London, 137 (6): 692 (1932).
- [18] C. Wittig, J. Phys. Chem. B 109, 8428 (2005).
- [19] S. Teufel, "Adiabatic Perturbation Theory in Quantum Dynamics", (Springer, Berlin, 2003).

- [20] S. Schmidt, D. Blaschke, G. Röpke, S.A. Smolyansky, A.V. Prozorkevich and V.D. Toneev, Int. J. Mod. Phys. E 7, 709 (1998).
- [21] Y. Kluger, E. Mottola and J.M. Eisenberg, Phys. Rev. D 58, 125015 (1998).
- [22] J.C.R. Bloch, V.A. Mizerny, A.V. Prozorkevich, C.D. Roberts, S.M. Schmidt, S.A. Smolyansky and D.V. Vinnik, Phys. Rev. D 60, 116011 (1999).
- [23] R. Alkofer, M.B. Hecht, C.D. Roberts, S.M. Schmidt and D.V. Vinnik, Phys. Rev. Lett. 87, 193902 (2001).
- [24] C. Kohlfürst, M. Mitter, G. von Winckel, F. Hebenstreit and R. Alkofer, Phys. Rev. D 88, 045028 (2013).
- [25] C. Kohlfürst, Master's thesis, Graz University (2012), arXiv:1212.0880.
- [26] For a nice review, see, e.g., G.V. Dunne, "Heisenberg-Euler effective Lagrangians: Basics and extensions: Lectures Notes", in "From Fields to Strings: Circumnavigating Theoretical Physics", M. Shifman et al (ed.), 445-522 (Ian Kogan Memorial Collection, 2004), also published in hep-th/0406216.
- [27] G. Nenciu, Commun. Math. Phys. 76, 117 (1980).
- [28] P. Pickl and D. Dürr, Commun. Math. Phys. 282, 161 (2008) and Phys. Lett. 81, 40001 (2008).
- [29] F. Beck, "Adiabatic pair creation", Thesis (2013), see also, http://www.mathematik.uni-muenchen.de/%7Ebohmmech/theses/Beck Franziska BA.pdf